Int J Adv Manuf Technol
DOI 10.1007/s00170-017-0338-6

ORIGINAL ARTICLE

Modelling the flash formation of linear friction welded 30CrNiMo8 high strength steel chains

P. S. Effertz[1] · **F. Fuchs**[2] · **N. Enzinger**[1]

Received: 22 February 2017 / Accepted: 23 March 2017

Abstract Linear friction welding (LFW) is a solid-state welding process and its initial purpose lies solely on the production of "blisks" for the aerospace industry. However, in recent years, the usability of LFW has expanded and gained the interest from various industries regarding near-net-shapes. Also in chain manufacturing, LFW has acquired interest over the more common flash butt welding (FBW) process. In this work, numerical modelling is used to study and understand the mechanisms responsible for the flash formation in a 30CrNiMo8 high strength steel chain. To that end, 2D computational modelling was considered using the finite element analysis (FEA) software DEFORM and was divided into two distinct approaches: a purely thermal model and a plastic flow model. Temperature measurements were carried out to validate the model and self-cleaning ability of the process was analyzed.

Keywords Linear friction welding · Numerical modelling · 30CrNiMo8 steel

1 Introduction

The joining process of steel chains has been carried out so far by flash butt welding (FBW) [1]. This process has been in use for many years and is successfully applied for different profiles and dimensions of chain links. However, this process yields low production, due to relatively long cycle time. Also, due to the heat input of this low energy density fusion welding process, the material becomes liquid, and the microstructure is influenced significantly in a wide heat affected zone (HAZ) and makes post-weld heat treatment (PWHT) and an expensive quality control necessary [1]. Welding defects related to fusion joining processes, such as slag residues, porosity, segregation or hot cracking can appear [1–2]. To overcome the shortcomings related to FBW, linear friction welding (LFW) is a subject of research in chain welding in the recent years, since it guarantees very clean and reproducible welds, comprising exceptional mechanical properties [3].

LFW is a solid-state joining process in which the bonding of two components is accomplished by their relative reciprocating motion under axial compressive forces [4–5]. Although the process is continuous, LFW can be split into four phases [6–9].

In the *initial phase*, the two surfaces are brought into contact under external load. Interaction between the surface asperities occurs, thus, generating heat due to friction. The asperities soften and deform, increasing the true contact area between the two workpieces. In this phase, negligible axial shortening (burn-off) perpendicular to the oscillation direction is observed.

1. In the *transition phase*, the material plasticizes and becomes viscous, causing the true contact area to increase until total surface contact is established. Heat from the interface is conducted to its vicinity, plasticizing more material, and burn-off starts to occur as a result of the expulsion of viscous material.
2. At this point, the force, thermal profile and burn-off reach a quasi-steady-state condition, and significant burn-off occurs through the rapid expulsion of viscous material

✉ P. S. Effertz
pedro.effertz@tugraz.at

[1] Institute of Materials Science and Welding, Graz University of Technology, Kopernikusgasse 24/I, 8010 Graz, Austria

[2] pewag austria GmbH, Mariazeller Straβe 143, 8605 Kapfenberg, Austria

Published online: 03 April 2017

trough the interface. This phase is referred as the *equilibrium phase.*

3. Finally, during the deceleration phase, the motion is ceased in a quick, however, progressive manner, to ensure alignment between the workpieces. At that time, the axial force is increased to forge the two components together, which give this phase its name: *forge phase*

Due to the rapid nature of the LFW process, computational modelling is used to understand what is happening during the process and characterize its evolution. Various authors developed 2D [4, 6, 10–12] and 3D [13–17] computational models in order to predict various welding outputs, such as thermal fields [12, 18–20], flash morphology and formation rates [10, 13, 19, 21], residual stresses, strain rates [10] and microstructural characterization [22].

According to literature, 2D models prove to give good insight to the process without the drawback of high computational times comprised in 3D models. Three main approaches are used by various authors when modelling the LFW process.

One approach is to model two separate workpieces where one of them is oscillating, as it is coupled with an oscillating tool and the other applies the axial force and is also matted to a forging tool, as shown in Fig. 1a [4, 19, 23]. This allows the entire process to be modelled. Nevertheless, the friction coefficient needs to be known in order to reproduce accurately the thermal aspects in the initial phase of the process. In addition, with this approach, the workpieces do not merge, unlike what happens in reality.

Another approach is to model only one workpiece that oscillates against a non-deformable object, as presented in Fig. 1b [11, 12, 17, 24]. Once more, this approach requires information on the friction conditions on the interface and does not consider mechanical mixing.

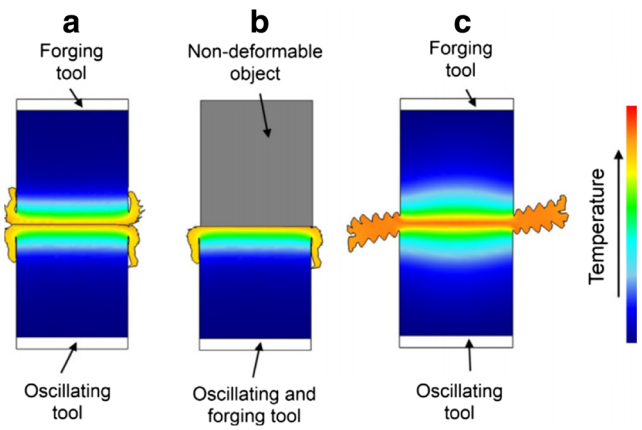

Fig. 1 Modelling approaches. **a** Two workpieces. **b** One workpiece and a non-deformable tool. **c** A single body representing two workpieces [6]

Finally, for the third approach, a single body representing two workpieces is considered that sticking friction takes place and 100% of true contact at the interface. A temperature profile needs to be put onto the single body that accounts for the heat generated by sliding friction. The high temperatures in the interface results in high viscosity of the material in the weld interface of the model. By considering the adhesion in this region, the model is able to simulate the recrystallization of the separate workpieces. Thus, better modelling of the flash formation and its morphology is achieved. However, the limitations inherent to this approach have to do with the fact that all stages prior to sticking conditions are not able to be modelled [6, 9, 10, 21].

The present work focuses on a weakly coupled numerical model as a way to comprehend the welding process applied specifically to chains. The importance of this study lies in the advantage of predicting some of the intervening physical quantities of the process, such as temperature distribution, flash formation and shortening. Further on, the effect of different welding parameters can be estimated. The work from other authors investigates grossly Ti64 on the scope of aerospace applications. Furthermore, in all FW modelling activities, the heat input is a question of research with special focus on friction. In this contribution, this topic is dealt by estimating the transient heat input by the work load of the FW device, comparable to the work presented in previous investigations. However, a different material is considered (in own experiments, it was observed that changing the materials can lead to a complete different behaviour).

2 Methodology

2.1 Experimental procedure

The material used for the experiments was 30CrNiMo8 which is widely used for highly stressed components in the aerospace and automotive industries. The mechanical properties at room temperature show a yield strength and tensile strength of 1050 and 1550 MPa, respectively, and a total fracture elongation of 9%. Dropforged half chain links with a cross section of 22 mm in width and 24 mm in height were used for the welding experiments in a prototype welding machine. The apparatus is fully instrumented and allows the measurement of both normal and in-plane forces as well as displacements during the process.

In LFW, the main process parameters are the frequency of oscillation f, the amplitude of oscillation a, and the applied load L during friction and forging stage [5, 25]. For the present work, it is already known that the

combination of parameters which yield the best mechanical properties, thus, only one combination was studied. The oscillation direction is parallel to the 24-mm height of the cross section, thus, perpendicular to the 22 mm of the cross section width.

Post-welding analysis was carried out using optical microscopy, specifically to characterize the geometry of the flash and compare with the results yielded by the numerical model. After embedding in cold resin, the sample was ground using SiC papers from 120 grit to 4000. After grinding, the sectioned sample was polished with 3 and 1 μm of OPS suspension. The sample was then etched using Nital 5%.

Thermocouple measurements were performed to validate the data provided by the thermal model. To install the k-type thermocouples (ø0.3 mm), one of the links was cut in half, and three channels (ø2.5 mm) were milled perpendicular to the oscillation direction and parallel to the axial loading direction, to accommodate the wiring. The equally distance channels were milled until 3.6, 4 and 4.8 mm from the interface. To secure the terminals in place, epoxy resin was used. The described set-up is shown in Fig. 2. Finally, the two halves were joined together and locally TIG welded as far away as possible from the weld interface, to avoid subjecting regions around the interface to thermal cycle and ensure their alignment throughout the process.

2.1.1 Energy input analysis

The energy going into each weld can be determined from the load cell and displacement measurements made by the machine during each welding experiment. However, the load is not being measured at the sample but rather between the clamping tool and a servo hydraulic actuator. To determine the energy put into the weld, one has to know the force at the sample interface given by F_{int} as shown in Fig. 3 [26]. Thus, the instantaneous power that goes into the sample can be computed by

$$q = F_{\text{int}}^{\text{net}}(t)v(t) \tag{1}$$

The total energy inputted to the weld interface during a certain time span can be obtained by integrating Eq. 1 over the phase duration t_x

$$E_x = \int_0^{t_x} q dt \tag{2}$$

Applying free body analysis to the system presented in Fig. 3, the load in the interface can be computed by

$$F_{\text{int}} = F_1 - Ma \tag{3}$$

However, the mass M of the oscillating system is unknown. Therefore, the LFW machine was subjected to a "dry run" to account for the inertial movement of the tooling system F_{int}^0. The load registered was then subtracted to the results obtained when the machine is loaded with a sample $F_{\text{int}}^{\text{net}} = F_{\text{int}}^{\text{total}} - F_{\text{int}}^0$. The preceding analysis requires an estimate of the velocity. This can be achieved numerically, since the position at discrete values in time is known. Thus, the central finite difference is used for the first order derivative [27],

$$v_1 = \frac{x_{t+\Delta t} - x_{t-\Delta t}}{2\Delta t} \tag{4}$$

where v_1 is the velocity at the present time level, $x_{t+\Delta t}$ and $x_{t-\Delta t}$ are the position at the previous and future time levels, respectively. Δt denotes the time step size.

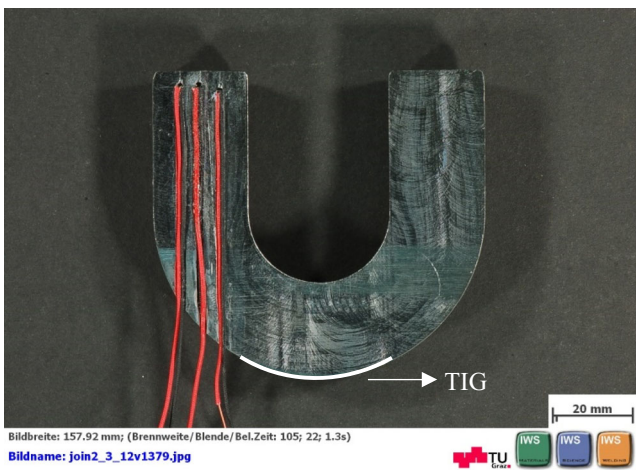

Fig. 2 Macrograph with the positioning of the k-thermocouples: 3.6 mm (*left*), 4.0 mm (*center*) and 4.8 mm (*right*) from the interface. The tack welding position is indicated by the *white line*

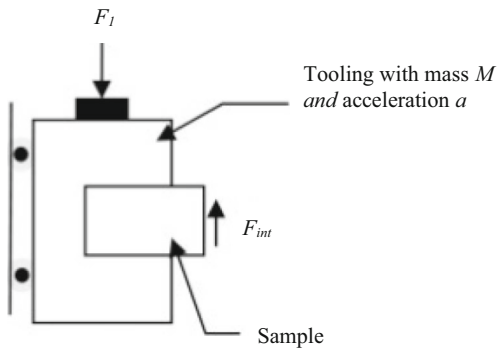

Fig. 3 Schematic diagram of the oscillating mechanism of an LFW machine [26]

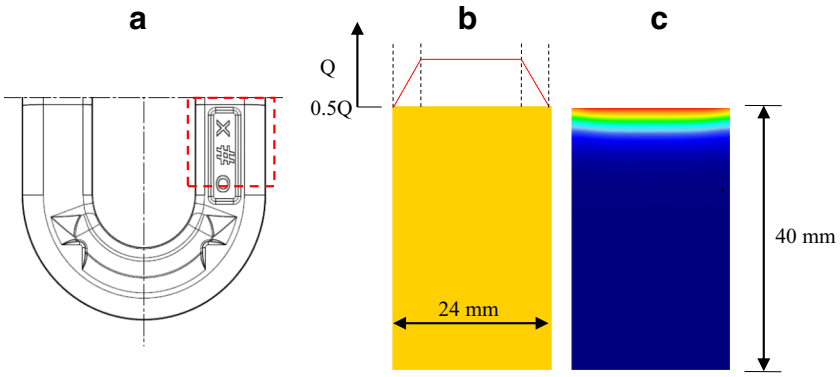

Fig. 4 2D thermal model. **a** Region of interest. **b** Heat flux approach used. **c** Thermal profile generated at the end of the initial phase

2.2 Numerical model

Numerical modelling was carried out, with the aim of predicting the material flow phenomena accurately. To that end, the models were developed with finite element analysis (FEA) using DEFORM. Due to the complexity of the LFW process, several simplifying assumptions were adopted. Firstly, the modelling was carried out in 2D as plain strain, where no deformation normal to the oscillation direction is considered. Secondly, three modelling approaches presented in Fig. 1c were considered. Thus, the process was divided into two distinct stages. The first stage consists in a purely thermal model to represent the heating by friction in the initial phase, and the second stage was used to account for plastic deformation in the transition and equilibrium phase by means of a thermomechanically coupled model. However, unlike the work reported by other authors, the initial phase in the present work has considerable plastic deformation and is traduced in approximately 2 mm of burn-off. This has to do with the fact that the interface of the chains is not flat. Due to the forging process, the interface of the chain has a ridge, and the edges are round. However, for the present study, the deformation on the initial phase was not considered. The models were ran until a burn-off of 4 mm was reached, representing the remaining burn-off from transition and equilibrium phases.

2.2.1 Thermal model

The thermal model was developed having into consideration previous works developed by [6, 18], in order to give insight on how 2D models can be used to estimate the heating during the initial phase of the process. The temperature-dependent thermal conductivity and specific heat used were based on empirical data [28]. Emissivity values were kept in DEFORM default settings. Ambient temperature and initial workpiece temperature were set to 30 °C. Convective heat transfer was assumed to be 20 W/(m^2 K). The dimensions of the modelled test piece are consistent with the experiment in terms of width. However, only a small portion of the chain link height was considered, as depicted in Fig. 4a. For this heating

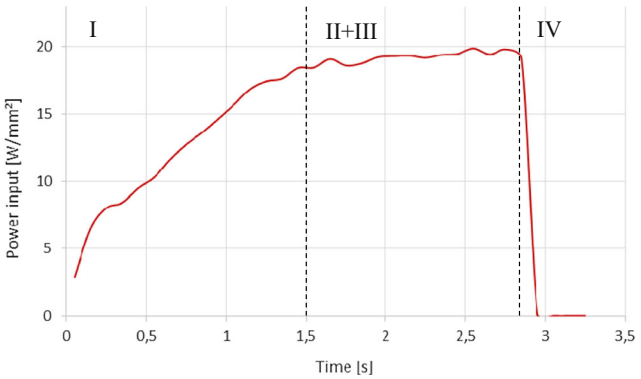

Fig. 5 Power input per phase at the interface. Each phase separated by the dashed lines. *I* initial phase, *II* + *III* transition and equilibrium phases, *IV* forging phase

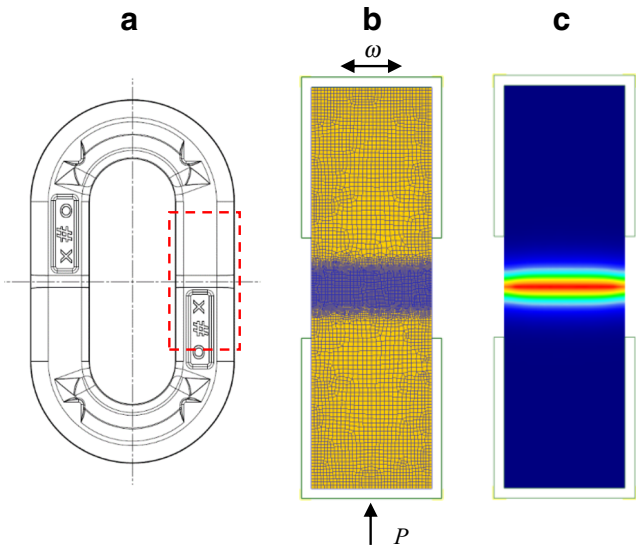

Fig. 7 2D Plastic flow model. **a** Region of interest. **b** Illustration on the setup of the plastic flow model, mesh and boundary conditions. **c** Thermal profile mapped onto the plastic flow model

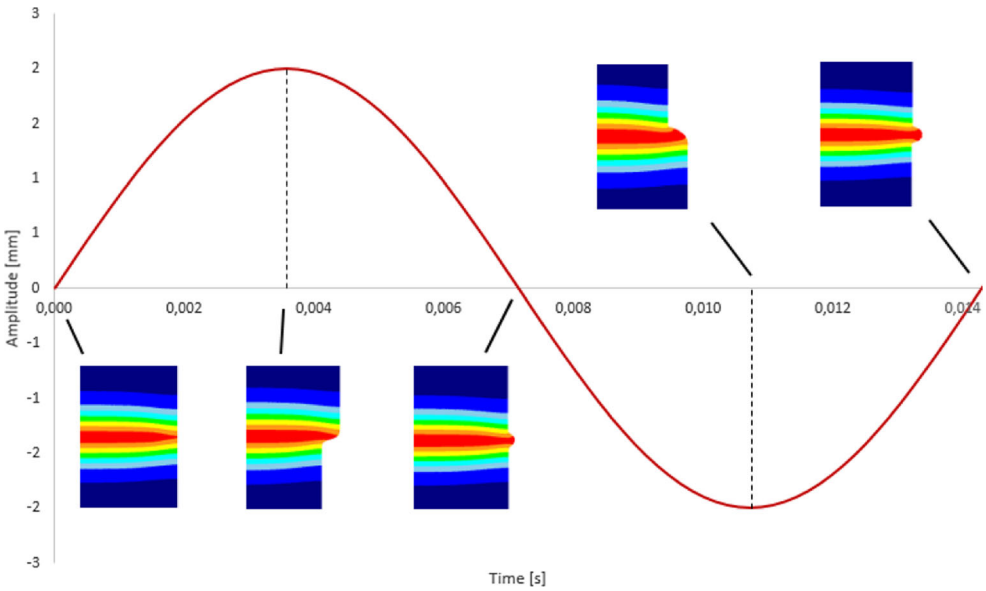

Fig. 8 Flash formation in the early stages of the LFW modelling during one oscillation cycle

model, no dies where used. Three different mesh windows were considered. For the region containing the weld interface, element size of 0.2 mm was used.

As reported in [18], a uniform heat flux (Q) was applied across most of the interface and lineally reduced to 50% of this value from a distance away from the edge, corresponding to the amplitude. This reduction represents the effect of the oscillatory movement, where the offset between the workpieces means a lower heat input in the regions of the edges (see Fig. 4b). The total energy put into the weld interface for a specific phase can be determined by Eq. 2 [6, 26]. Figure 5 depicts the power input in the middle section of the interface per phase. It can be acknowledged that the power input is constant throughout the transition and equilibrium phases. This might suggest that the interface surface has even out becoming flat and in total contact.

The interface temperature has been shown to be approximatelly 950 °C according to [17]. Thus, the heat flux in the initial phase was applied until 1.5 s, guaranteeing that all elements reach this temperature.

2.2.2 Thermomechanical model

The single body model uses a 2D deformable workpiece in plane strain condition, representing the central slice of one half on the chain link, as depicted in Fig. 7. The oscillatory movement and axial loading is generated by two rigid tools. The aforementioned thermal profile was mapped onto the plastic flow model, as shown in Fig. 7c.

Most of the heat generation and plastic deformation throughout the process occurs along the weld interface. Thus, an average element size of 0.2 mm was used within a 10 mm band around the interface. Outside this region, as the distance increases, the element size also increases. Material flow stress data was previously characterized with compression tests at different temperatures, in order to obtain the viscoplastic behaviour of the material [28].

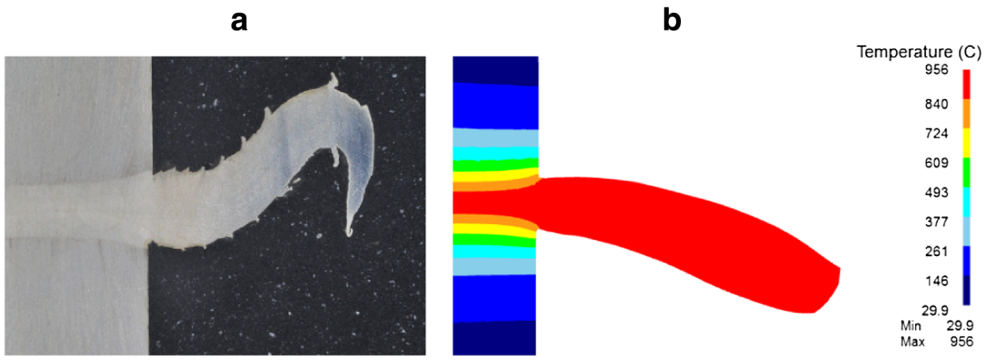

Fig. 9 Flash morphology comparison between the **a** experimental and **b** model

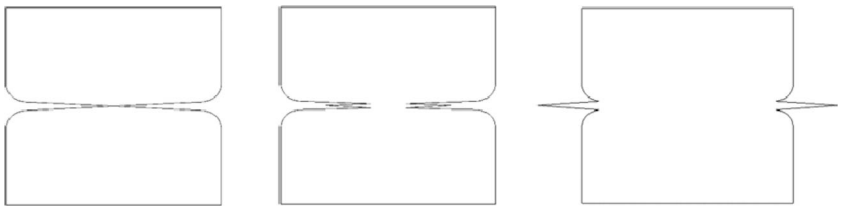

Fig. 10 Schematic representation of the evolution of the flash formation at the interface of the chain

Temperature-dependent thermal conductivity, specific heat and emissivity values used were identical to the thermal model. Ambient temperature was assumed to be 30 °C.

A time-step of 9×10^{-5} s was used to ensure only a half of the element thickness was travelled during the reciprocating motion.

3 Results and discussion

3.1 Flash formation

Turner et al. [10] studied the flash formation mechanisms and its morphology in order to test the accuracy of the modelling. It was found that the shape and formation of the flash produced reflects the mechanisms driving deformation. Viscous material is expelled according to two main mechanisms. The first effect is due to the oscillatory motion dragging the material from the weld line during each oscillation stroke. When the offset between the workpieces is at its maximum value, the in-contact area is lower, which leads to a pressure increase. Cooler material will therefore be plunged into the highly viscous material. Thus, while the workpieces return to the aligned position, the viscous material shears past the edge of the workpiece, generating the flash. The second is related to the forging load steadily extruding the plasticized material from the weld line. The mechanism which prevails is related to the parameter values used. For welds produced with smaller amplitudes, the second mechanism aforementioned is the most influential. On the other hand, for larger amplitudes, the morphology is dominated by the oscillations which drag the material out from the weld, producing a rippling pattern. Each ripple is related to one oscillation.

For the present study, the amplitude is not able to shear the material. Hence, the second mechanism occurs, and the extruded material remains in constant contact with the upper and lower workpiece during oscillation. Figure 8 depicts the flash formation mechanism in the beginning of the LFW process over one complete cycle. The reason to evaluate has to do with the fact that, in the beginning, the thermal profile might not be thick enough to accommodate the difference in strain rates between the interface and material being sheared by the edge. However, for this particular case, the flash remains in contact with the edges of the workpieces, and the approximate strain rate is 1100 s^{-1}. As a result, smooth and wide flash without distinctive ripple is formed.

Figure 9 depicts the comparison between the experimental and modelling results for the flash morphology. Although the experimental flash is characterized by a smooth surface, there is small rippling which has not been reproduced by the model. Also, the predicted flash shows a rounded edge, in contrast with the sharp edge obtained in the experiment. This difference is due to the fact that in the beginning of the welding process, the interface of the chain is not flat.

This traduces in higher pressure and local heat input, consequently plasticizing locally the material in the interface (see

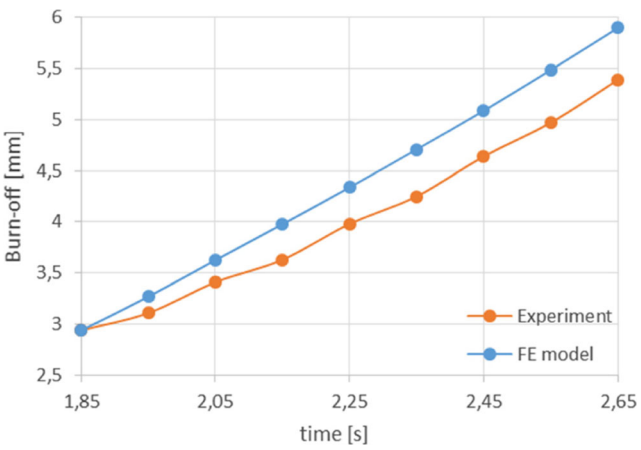

Fig. 11 Experimental and predicted burn-off as a function of time

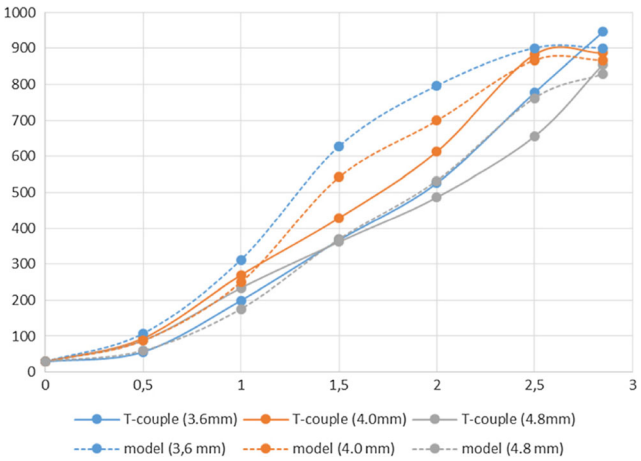

Fig. 12 Comparison of the thermal histories between the FEA and experiment

Fig. 13 Illustration of the evolution of the surface contaminants using point tracking. **a** Initial positioning of the points on the weld line. **b** Points are being extruded through the flash.**c** Contaminants completely removed

Fig. 10). Finally, the flash deflects upwards and downwards with the reciprocating movement, reaching its maximum height when the amplitude is at its maximum value. At a certain length, the flash makes contact with the tooling, causing it to bend as shown in Fig. 9a.

3.2 Burn-off rate

It is of interest to study the material that is expelled from the weld as flash, since its volume represents a direct contribution to the upsetting process. Thus, predicting the rate of formation of the flash is of great importance. The model predicted a linear axial shortening, typical of the LFW process in the equilibrium stage, where quasi-steady state conditions are achieved. Figure 11 relates the burn-off as a function of time for the experiment and model. The gradient of the model and experimental curve yields a burn of rate of 3.67 and 3.08 mm s^{-1}, respectively. The slight discrepancy between the experimental and predicted burn-off rate might be due to an excessively hot temperature profile, which traduces in a higher viscoplastic flow. Nevertheless, the good agreement supports the adequacy of the material model used.

3.3 Thermal validation

The thermal histories shown were taken at every 0.5 s at the upset position recorded by the machine, as presented in Fig. 12. The predicted temperatures are presented until the end of the equilibrium phase. A fairly good match was obtained for the purely thermal model and thermocouple recordings for initial and equilibrium phases. Intuitively, the recordings made by the thermocouple closest to the interface should record the highest temperature, which does not occur with the 3.6 mm one. In the first 1.5 s, this thermocouple is recording lower temperatures than the one furthest away and is also below the 4.0 mm thermocouple almost throughout the whole process. Thus, the validity of the recordings of this particular thermocouple can be considered as questionable. This statement can be supported by the reasonable agreement between the experiment and model for the 4.0 and 4.8 mm readings. Despite this, further temperature measurements should be carried out.

A slight discrepancy is present in the 4.0 mm between 1.5 and 2 s, which confirms excessive heating provided by the purely thermal model, already acknowledged in the previous section.

3.4 Self-cleaning effect

To determine whether the present combination of welding parameters provides a weld free of surface contaminants, point tracking provided by DEFORM was used along the interface, similar to the work reported by Turner et al. [10] and McAndrew et al. [6, 9]. Weld line self-cleaning is an important matter, since the present of surface oxides or other contaminants compromise the mechanical properties of the welded chains. Figure 13a shows the displacement of the tracking points, each separated by 2 mm. Modelling demonstrated that throughout the weld, the unwanted contaminants are expelled, providing that a sufficiently large number of oscillations and burn-off is used (see Fig. 13b, c).

4 Conclusions

This work reported the initial investigation to the linear friction welding of a 30CrNiMo8 high strength steel chain using a 2D FEA approach. The following conclusions can be drawn from this work:

A finite element modelling for the LFW of 30CrNiMo8 high strength steel chains has been formulated, using well-known parameters, in order to predict the thermal and mechanical characteristics of the process by means of purely thermal and thermomechanical models. A very good agreement between reality and model was achieved without application of a single fit parameter.

The uneven interface surface of the chains is responsible for the plastic deformation present in the initial phase of the process. This phenomenon is not reproducible in the purely thermal model.

Flash showed a smooth morphology much in accordance with experimental observation apart from the slight rippling effect of this last one. This smooth pattern is related to low process parameters which yield low energy input. The local plasticization of the material due to the uneven surface of the interface meant that the morphology of edges between experimental and predicted flash did not match. The mechanism that prevails for the set of parameters in this study is dictated

by the forging load, steadily extruding viscous material from the interface.

The burn-off rate in the equilibrium phase yielded from the model is considerably higher than the experiment. This is probably due to the excessively high temperature assumed in the interface of the model, consequently leading to rapid viscoplastic flow.

Temperature history produced by the model proved to be reliable according to the results obtained by the temperature measurements, with exception for the thermocouple located initially at 3.6 mm from the interface. However, the slight disagreement between model and experiment at 4.0 and 4.8 mm from the interface were attributed to the displacement of the thermocouples from their expected positioning by the plasticized material.

The process showed self-cleaning properties along the weld line, meaning that all surface asperities are completely expelled from the interface trough the flash, as long as the process is provided with enough burn-off.

Acknowledgements The authors gratefully acknowledge the financial support of this work by the project JOIN. The K-Project Network of Excellence for Joining Technologies JOIN fostered in the frame of COMET—Competence Centers for Excellent Technologies by BMVIT, BMWFJ, FFG, Land Oberöstereich, Land Steiermark, SFG and ZIT. The program COMET is handled by FFG.

References

1. K. Mucic, N. Enzinger, and F. Fuchs, "Linear Friction Welding of High Strength Chains," *Trends Weld. Res. Proc. 9th Int. Conf.*, pp. 752–756, 2013.
2. Çetinkaya C, Arabaci U (2006) Flash butt welding application on 16MnCr5 chain steel and investigations of mechanical properties. Mater Des 27(10):1187–1195
3. K. Mucic, F. Fuchs, and N. Enzinger, Process optimization for linear friction welding of high strength chain, in *EUROJOIN Conference*, 2012, pp. 157–166.
4. Song X, Xie M, Hofmann F, Jun TS, Connolley T, Reinhard C, Atwood RC, Connor L, Drakopoulos M, Harding S, Korsunsky AM (2013) Residual stresses in linear friction welding of aluminium alloys. Mater Des 50:360–369
5. Bhamji I, Preuss M, Threadgill PLL, Addison ACC (2011) Solid state joining of metals by linear friction welding: a literature review. Mater Sci Technol 27(1):2–12
6. A. R. McAndrew, P. A. Colegrove, A. C. Addison, B. C. D. Flipo, and M. J. Russell, Modelling the influence of the process inputs on the removal of surface contaminants from Ti-6Al-4V linear friction welds, *Mater. Des.*, vol. 66, no. PA, pp. 183–195, 2015.
7. Vairis A, Frost M (1998) High frequency linear friction welding of a titanium alloy. Wear 217(1):117–131
8. Vairis A, Frost M (1999) On the extrusion stage of linear friction welding of Ti 6Al 4V. Mater Sci Eng A 271(1–2):477–484
9. A. R. Mcandrew, 2D linear friction weld modelling of a Ti-6Al-J estr, no. September 2015, pp. 4–9, 2016.
10. Turner R, Gebelin JC, Ward RM, Reed RC (2011) Linear friction welding of Ti-6Al-4V: modelling and validation. Acta Mater 59(10):3792–3803
11. Vairis A, Frost M (2000) Modelling the linear friction welding of titanium blocks. Mater Sci Eng A 292(1):8–17
12. Li W-Y, Ma T, Li J (2010) Numerical simulation of linear friction welding of titanium alloy: effects of processing parameters. Mater Des 31(3):1497–1507
13. Sorina-Müller J, Rettenmayr M, Schneefeld D, Roder O, Fried W (2010) FEM simulation of the linear friction welding of titanium alloys. Comput Mater Sci 48(4):749–758
14. Buffa G, Cammalleri M, Campanella D, Fratini L (2015) Shear coefficient determination in linear friction welding of aluminum alloys. Mater Des 82:238–246
15. Mao Y, Ke L, Liu F, Liu Q, Huang C, Xing L (2014) Effect of tool pin eccentricity on microstructure and mechanical properties in friction stir welded 7075 aluminum alloy thick plate. Mater Des 62:334–343
16. Gao Z, Niu JT, Krumphals F, Enzinger N, Mitsche S, Sommitsch C (2013) FE modelling of microstructure evolution during friction stir spot welding in AA6082-T6. Weld World 57(6):895–902
17. Li W, Wang F, Shi S, Ma T, Li J, Vairis A (2014) 3D finite element analysis of the effect of process parameters on linear friction welding of mild steel. J Mater Eng Perform 23(11):4010–4018
18. McAndrew AR, Colegrove PA, Addison AC, Flipo BCD, Russell MJ (2014) Energy and force analysis of Ti-6Al-4V linear friction welds for computational modeling input and validation data. Metall Mater Trans A Phys Metall Mater Sci 45(13):6118–6128
19. Ceretti E, Fratini L, Giardini C, La Spisa D (2010) Numerical modelling of the linear friction welding process. Int J Mater Form 3(SUPPL. 1):1015–1018
20. Turner R, Ward RM, March R, Reed RC (2012) The magnitude and origin of residual stress in Ti-6Al-4V linear friction welds: an investigation by validated numerical modeling. Metall Mater Trans B Process Metall Mater Process Sci 43(1):186–197
21. F. Schroeder, R. M. Ward, R. P. Turner, M. M. Attallah, J. Gebelin, and R. C. Reed, Linear friction welding of titanium alloys for aeroengine applications: modelling and validation, *9th Int. Conf. Trends Weld. Res.*, no. January, pp. 886–892, 2012.
22. Grujicic M, Yavari R, Snipes JS, Ramaswami S, Yen CF, Cheeseman BA (2014) Linear friction welding process model for carpenter custom 465 precipitation-hardened martensitic stainless steel. J Mater Eng Perform 23(6):2182–2198
23. Fratini L, Buffa G, Campanella D, La Spisa D (2012) Investigations on the linear friction welding process through numerical simulations and experiments. Mater Des 40:285–291
24. Yang X, Li W, Li J, Xiao B, Ma T, Huang Z, Guo J (2015) Finite element modeling of the linear friction welding of GH4169 superalloy. Mater Des 87:215–230
25. Maalekian M (2007) Friction welding—critical assessment of literature. Sci Technol Weld Join 12(8):738–759
26. Ofem UU, Colegrove PA, Addison A, Russell MJ (2010) Energy and force analysis of linear friction welds in medium carbon steel. Sci Technol Weld Join 15(6):479–485
27. E. Kreyszig, *Advanced Engineering Mathematics: Maple Computer Guide*, 8th ed. New York, NY, USA: John Wiley & Sons, Inc., 2000.
28. M. Stummer, "Eigenschaften von 30CrNiMo8 für die Simulation," TU Graz, 2014.